

Article ID 1004-924X(2007)12-1844-06

# 上海光源真空紫外角分辨光电子能谱束线设计

马德伟, 乔 山, 张新夷, 封东来

(复旦大学 物理系 应用表面物理国家重点实验室, 上海 200433)

**摘要:** 在上海光源上设计了一条光子能量覆盖 5~140 eV 的高通量、高分辨的真空紫外角分辨光电子能谱束线。本光束线采用准周期椭圆偏振振荡器光源, 其周期长度为 0.32 m, 周期数为 14。单色仪采用 Dragon 型, 分为覆盖 5~32 eV 的低能分支和 25~140 eV 的高能分支。计算表明, 当入射/出射狭缝开启宽度为  $5/5 \mu\text{m}$  时, 在整个能量扫描范围内, 单色仪分辨率可以高达 15 000~100 000, 光学元件的面型误差对分辨率的影响最大。通量计算显示, 样品处 s 偏振光子通量高达  $\sim 10^{12}$  phs/s。Shadow 追迹模拟结果表明, 设计的光束线具有很好的聚焦特性。

**关键词:** 光束线设计; 真空紫外; 高分辨; 高通量

中图分类号: O657.62; TH838.3 文献标识码: A

## Design of VUV beamline for ARPES studies at SSRF

MA De-wei, QIAO Shan, ZHANG Xin-yi, FENG Dong-lai

(State Key Laboratory of Applied Surface Physics, Department of Physics,  
Fudan University, Shanghai 200433, China)

**Abstract:** Vacuum ultraviolet (VUV) beamlines have been playing an important role in studying the electronic structure of solids. Until now, over 30 VUV beamlines for Angle-resolved Photoemission Spectroscopy (ARPES) studies have been built in the synchrotron radiation facilities of US, Japan and Europe. In this work, we present a design of a high-resolution and high-flux VUV beamline covering 5~140 eV photon energy range at Shanghai Synchrotron Radiation Facility(SSRF) for ARPES studies. A quasi-periodic Elliptical Polarized Undulator (EPU) with 14 periods and each 0.32 m long is used as the source. A Dragon-type monochromator with two branches, a lower energy branch covering 5~32 eV and a higher one covering 25~140 eV, is employed. Calculations show that the total resolutions of the monochromator can reach up to 15 000~100 000 with entrance/exit slit openings of  $5/5 \mu\text{m}$  and the ultimate flux of the s-polarized photon on a sample exceeds  $\sim 10^{12}$  phs/s. The figure slope errors dominate the total resolution limit of the monochromator. Ray-tracing simulations show that the designed beamline has a good focusing performance. This beamline will be the first VUV beamline constructed at SSRF and will provide valuable experience for future constructions.

**Key words:** beamline design; VUV; high resolution; high-flux

**Received date:** 2007-08-20; **Revised date:** 2007-10-10.

**Foundation item:** Supported by the Chinese Post-doctoral Science Foundation and the National Natural Science Foundation of China

## 1 Introduction

Over the past two decades, the vacuum ultraviolet (VUV) beamline and its Angle-resolved Photoemission Spectroscopy (ARPES) end-station have been playing important roles in studying the electronic structure of solids, and a great deal of work completed by this experimental facility has made a deep impact on the understanding of condensed matter physics<sup>[1-3]</sup>. For instance, the ALS10.0.1 beamline, co-invested and co-operated by Stanford University and Lawrence Berkeley National Laboratory, was considered to be the most productive material science beamline of the US Department of Energy in 2005. Until now, over 30 VUV beamlines for ARPES studies have been built in the synchrotron radiation facilities of US, Japan and Europe. However, there are few high-flux and high-resolution VUV beamlines, especially in the photon energy range of less than 30 eV in a medium energy ring.

The Shanghai Synchrotron Radiation Facility (SSRF), which is the third-generation light source with a high storage electron energy of 3.5 GeV ranked 4<sup>th</sup> in the world, will supply high photon flux for its beamlines, but meanwhile, it will produce a high thermal load which will result in large distortions on the surfaces of the optical elements and consequently undermine the normal operations. Moreover, aspects such as monochromator design and suppression of higher harmonics are also directly responsible for the beamline performance. Based on recent investigations and accurate calculations, we have designed a high-flux and high-resolution VUV beamline for ARPES studies at SSRF, which will be the first VUV beamline at SSRF. It will provide valuable experience for future beamline construction. In this paper, the design of this beamline is described.

## 2 Beamline descriptions

### 2.1 Source

A quasi-periodic Elliptically Polarized Undulator (EPU) will be installed in a medium straight section (6.5 m) labeled as BL04U1. The undulator has 12 main and 2 correction periods of magnets, each being 0.32 m long. The undulator can generate linearly polarized and circularly polarized photons of 5 ~ 140 eV in a standard mode or in a quasi-periodic mode through modulations of the magnetic fields. High spectral purity of the source is very important for our applications. The quasi-periodic undulator, which has been employed before to reduce higher harmonics and ensure high spectral purity with only a few percent intensity loss, seems able to fulfill this goal<sup>[4]</sup>. The calculated maximum total power emitted from the undulator is 1 670 W and the maximum power density is 2 740 W/mrad<sup>2</sup>, which are comparable to those of PLEIADES beamline at Soleil and BL21 beamline at the Taiwan Light Source. Using simulations with the ANSYS code, the downstream optical elements, especially the pre-focusing mirrors, can work quite well under such a heat load with an appropriate cooling mechanism.

### 2.2 Optical design

Fig. 1 shows the schematic layout of the beamline. At the end of the front-end region, a water-cooled four-jaws slit is used to define the horizontal and vertical acceptance angles of the beamline, which are 0.5 mrad × 0.5 mrad (h × v) and can accept over 86 % of the light.

A pair of Kirkpatrick and Baez (KB) mirrors is used as pre-focusing mirrors. The first mirror HFM, a cylindrical mirror coated with Au is placed vertically 20 m away from the centre of the undulator, and can realize the horizontal focusing of the source inside the storage ring. In addition, it acts as a high-frequency filtering

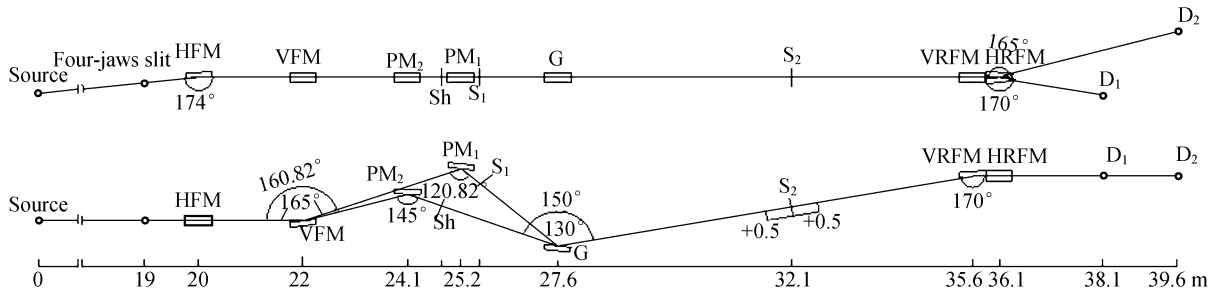


Fig. 1 Schematic layout of the beamline

mirror, cutting off the high energy radiation above 2 000 eV and absorbing most of the incoming thermal load. Thus it greatly reduces the heat on downstream optical elements. It also requires appropriate and efficient cooling system. The second mirror VFM is placed horizontally in order to deflect vertically and focus the incoming photon beam onto the entrance slits of the following monochromator.

The monochromator is the main optical element whose task is to disperse the incoming white light with the maximum transmission through the exit slit and with the minimum induced aberration. Here, a Dragon type monochromator with cylindrical gratings is chosen due to its simple wavelength scanning mechanism and desirable resolving power, which has been successfully realized in BL21 at the Taiwan Light Source<sup>[5]</sup>. Generally, for the design of this type of grating monochromator with minimum aberration, the defocusing term is the first one to be eliminated, that is,

$$\left(\frac{\cos^2 \alpha - \cos \alpha}{r_1} - \frac{\cos \alpha}{R}\right) + \left(\frac{\cos^2 \beta - \cos \beta}{r_2} - \frac{\cos \beta}{R}\right) = 0$$

where  $R$  is radius of the cylindrical grating,  $\alpha$  and  $\beta$  are the incoming and outgoing angles, respectively,  $r_1$  and  $r_2$  are the entrance and exit arm lengths respectively. Furthermore the primary coma, astigmatic coma and spherical aberration should be minimized.

The primary disadvantages of the Dragon design are: (1) the limited wavelength range covered by each grating; (2) the exit-slit needs

to move a relatively long distance, which induces large variations in the distance between the exit-slit and the refocusing mirror downstream, and the spot size on the sample<sup>[6-7]</sup>. In this scheme, we choose the monochromator length, the sum of the entrance and exit arm lengths, to be 6 m, and the translation distance of the exit arm length ranges from  $-400$  to  $+400$  mm along the optical axis, see Fig. 2. To match the movement of the exit-arm length, a bendable cylindrical mirror is used in the refocusing mirrors. By varying the meridional curvature radius of the mirror through bending, the focusing spot on the sample in a fixed position can be adjusted to minimal size.

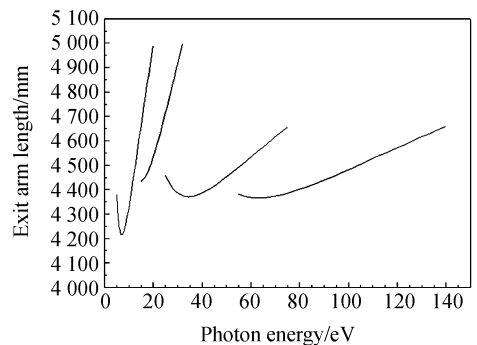


Fig. 2 Translation distance of exit arm length with photon energy

To cover the photon energy range of 5~140 eV, two branches are employed: a lower energy branch covering 5~32 eV and a higher one covering 25~140 eV, each one with two gratings. The two branches share the pre-focusing mirror VFM and the exit slit. The reflection and dif-

fraction efficiencies of the optical elements must be taken into account when considering the light beam transmission. The best way to design the monochromator is to optimize the diffraction efficiencies of the gratings for a given resolving power. Fig. 3 shows the optimized diffraction efficiencies of the gratings for this case. In this scheme, it is challenging to harmonize one branch with another to produce an optimally designed monochromator. The determined parameters of the monochromator and the calculated mirrors are shown in Tab. 1. The position marked  $D_1$  in Fig. 1 is for the ARPES end-sta-

tion, and the other branch  $D_2$  is reserved for future use.

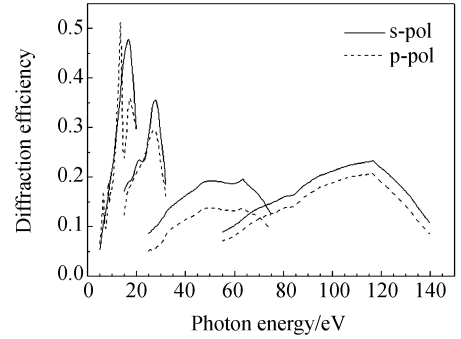


Fig. 3 Variation of the diffraction efficiency of the gratings with photon energy

Tab. 1 Parameters of the optical elements of beamline

Optical element	Shape	Substrate	Coating	Ruling density (1/mm)	Curvature radius(mm)	Deflection angle ( $^{\circ}$ )	Arm length $r_1$ $r_2$ (mm)	Slope error ( $\mu$ rad)
HFM	Cylinder	CVD-SiC	Au	-	215 074	174	20 000 7 832	1
VFM	Cylinder	CVD-SiC	Au	-	37 455	160.82/165	22 000 3 635/2 750	1
PM <sub>1</sub>	Plane	CVD-SiC	Au	-	$\infty$	120.82	3 174.7 460.3	1
PM <sub>2</sub>	Plane	CVD-SiC	Au	-	$\infty$	145	2 065.3 684.7	1
G <sub>1</sub>	Cylinder	CVD-SiC	Al+MgF <sub>2</sub>	900	7 400	130	1 940	1
G <sub>2</sub>	Cylinder	CVD-SiC	Al+MgF <sub>2</sub>	2 000	7 680		4 000~5 000	1
G <sub>3</sub>	Cylinder	CVD-SiC	Au	1 200	13 010	150	2 340	1
G <sub>4</sub>	Cylinder	CVD-SiC	Au	2 200	13 000		4 000~5 000	1
VRFM	Bendable Cylinder	glidcop	Au	-	31 292~ 45 895	170	3 000~4 000 2 500/4 000	2.5
HRFM	Cylinder	glidcop	Au	-	36 716/ 37 307	170/165	8 000 2 000/3 500	5

### 2.3 Performance calculations and ray-tracing

Fig. 4 shows the aberration including primary coma, astigmatic coma and spherical aberration limited resolution of the four gratings. The aberrations from the astigmatic coma and spherical aberration are considerably lower compared to that from the primary coma. Therefore, we only take account of the aberration from the primary coma in what follows.

To maximise the total resolving power of the monochromator, a convolution of aberration,

entrance slit, exit slit and figure slope error limited resolutions should be minimized. In this calculation, the vertical acceptances of the gratings are set at 2.5 mrad and the figure slope errors are listed in Tab. 1. Fig. 5 shows various resolution limits with an entrance to exit slit opening of 10/10  $\mu$ m, clearly the figure slope errors dominate the total resolution limits. In other words, the resolving power cannot be im-

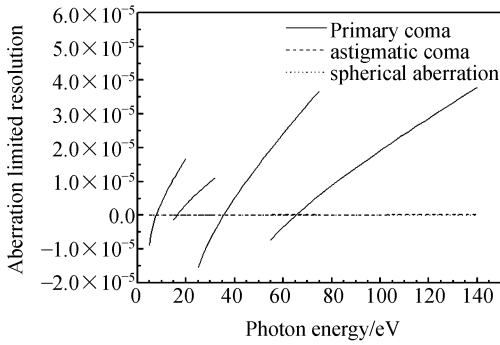


Fig. 4 Primary coma, astigmatic coma and spherical aberration limited resolutions

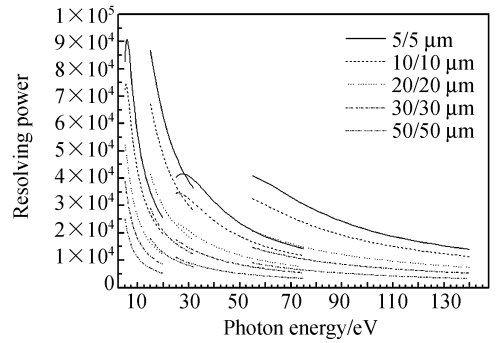


Fig. 6 Total resolutions with different slit opening settings

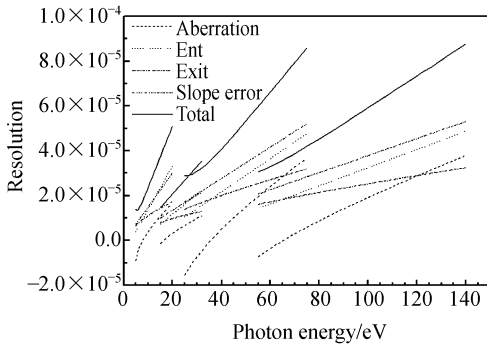


Fig. 5 Various resolution limits with entrance to exit slit openings of 10/10  $\mu\text{m}$

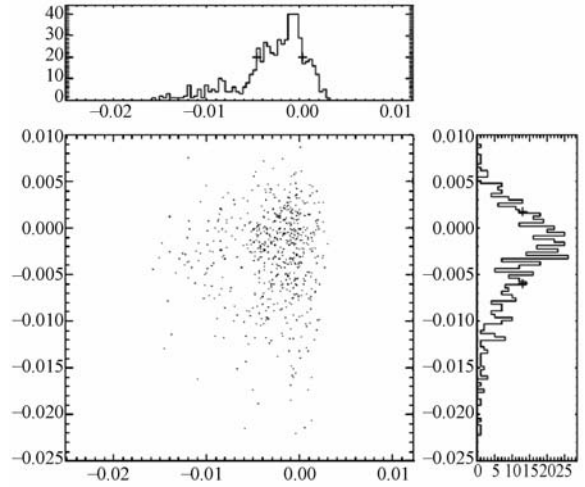


Fig. 7 Ray-tracing spot image on the sample; the spot size is about  $50 \mu\text{m} \times 77 \mu\text{m}$  ( $h \times v$ )

proved unless the figure error is reduced further.

Fig. 6 shows the total resolution of the monochromator with different slit opening settings. When the entrance to exit slit opening is set at  $5/5 \mu\text{m}$ , the resolving power reaches up to  $15\,000 \sim 100\,000$ . Even in the situation of slits wide open  $50/50 \mu\text{m}$ , which ensure that most photons in the entire scanning range pass through the slits, the resolving power is above  $5\,000$ .

Ray-tracing simulations are carried out by the Shadow code to examine the focusing performance of the beamline. Fig. 7 shows the ray-tracing pattern on the sample's position with photon energy of  $5 \text{ eV}$  and without the entrance and exit slits. The figure slope errors are also taken into account here (see Tab. 1). The full width at half maximum (FWHM) of the spot size is about  $50 \mu\text{m} \times 77 \mu\text{m}$ , indicative of a de-

sirable focusing performance. Fig. 8 shows the resolution observed at the position of the exit slit position with a  $10 \mu\text{m}$  entrance slit, up to  $670\,000$ , which is consistent with the above calculation.

The photon flux of the beamline is calculated with Spectra, XOP and Reflec codes. The surface roughness of all the optical elements is assumed to be  $0.3 \text{ nm}$ . Fig. 9 shows the calculated photon flux on the sample. The ultimate flux of s-polarized photons is over  $10^{12} \text{ phs/s}$ . However, the flux of p-polarized photons is relatively lower, especially in the energy range below  $30 \text{ eV}$ , the p-polarized photon flux is reduced by several orders of magnitude compared with the s-polarized flux. The design is in accordance with the expected target.

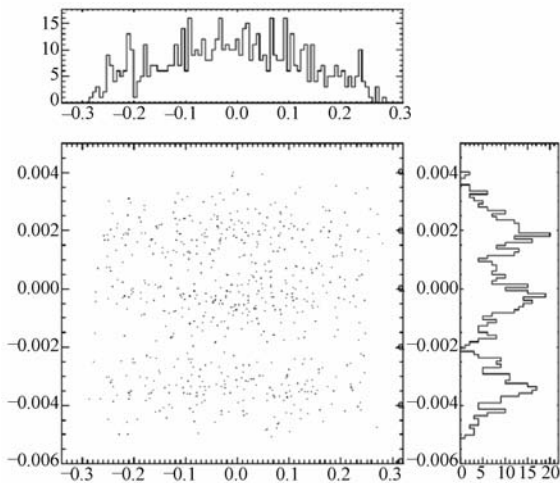


Fig. 8 Resolution observed at the position of the exit slit with an entrance slit opening of  $10 \mu\text{m}$ , the upper distance standing for  $E/\Delta E = 67\,000$  and the lower one for  $E/\Delta E = 50\,000$ .

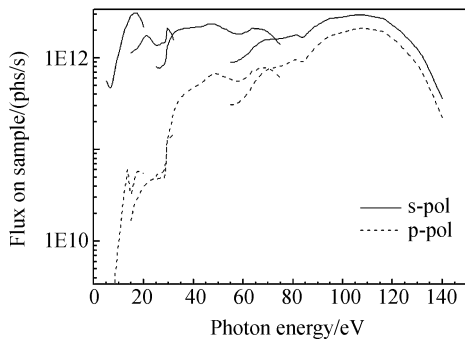


Fig. 9 Calculated photon flux on the sample

### 3 Conclusions

We have designed a high-resolution and high flux VUV beamline at SSRF for ARPES studies. A 6 m Dragon type monochromator with two branches is employed in this beamline. The translation distance of the exit arm length ranges from  $-400 \text{ mm}$  to  $+400 \text{ mm}$  along the optical axis, and a bendable cylindrical mirror is used in the refocusing mirrors in order to match the movement of the exit-arm length. After construction, this beamline will be a powerful research tool for condensed matter physics and materials scientists.

### 4 Acknowledgements

We would like to thank Professor Jianhua He, Renzhong Tai, Zhimin Dai and Naxiu Wang at SSRF for their invaluable comments and discussions concerning the beamline design.

### References:

- [1] TANAKA K, LEE W S, LU D H, *et al.*. Distinct fermi-momentum-dependent energy gaps in deeply underdoped Bi2212 [J]. *Science*, 2006, 314: 1910-1913.
- [2] TERASHIMA K, MATSUI H, HASHIMOTO D, *et al.*. Impurity effects on electron-mode coupling in high-temperature superconductors [J]. *Nature Physics*, 2006, 2: 27-31.
- [3] DAMASCELLI A, HUSSAIN Z, SHEN Z X. Angle-resolved photoemission studies of the cuprate superconductors [J]. *Reviews of Modern Physics*, 2003, 75: 473-541.
- [4] <http://sls.web.psi.ch/view.php/beamlines/sis/source/index.html>
- [5] SONG Y F, YUH J Y, LEE Y Y, *et al.*. Performance of an ultrahigh resolution cylindrical grating monochromator undulator beamline [J]. *Review of Scientific Instruments*, 2006, 77: 085102.
- [6] CHEN C T. Concept and design procedure for cylindrical element monochromators for synchrotron radiation [J]. *Nuclear Instruments and Methods A*, 1987, 256: 595-604.
- [7] PEATMAN W B. *Gratings, Mirrors and Slits: Beamline Design for Soft X-ray Synchrotron Radiation Sources* [M]. Netherlands: Gordon and Breach Science Publishers, 1977.

**Author's biography:** Ma De-wei (1975—), male, was born in Shandong Province of China. He received his PhD degree in 2004 from Zhejiang University. His research field involves synchrotron radiation beamline design & construction and material physics & chemistry. E-mail: dwma@fudan.edu.cn